PERFORMANCE OF THERMOELECTRIC COOLER POWERED BY PHOTOVOLTAIC CELL WITH AND WITHOUT COOLING METHOD

KUEK WEE EN

MASTER OF ENGINEERING (MECHANICAL)
(STRUCTURE C)

FACULTY OF ENGINEERING AND SCIENCE
UNIVERSITI TUNKU ABDUL RAHMAN
NOVEMBER 2021

PERFORMANCE OF THERMOELECTRIC COOLER POWERED BY PHOTOVOLTAIC CELL WITH AND WITHOUT COOLING METHOD

By

Kuek Wee En

A Thesis submitted to the Department of Mechanical & Material Engineering,
Faculty of Engineering and Science,
Universiti Tunku Abdul Rahman,
in partial fulfillment of the requirements for the degree of
Master of Mechanical Engineering by Coursework

ABSTRACT

PERFORMANCE OF THERMOELECTRIC COOLER POWERED BY PHOTOVOLTAIC CELL WITH AND WITHOUT COOLING METHOD

KUEK WEE EN

Solar powered thermoelectric refrigerator is a refrigerator that makes use of solar energy for electrical energy conversion to supply power to the thermoelectric module based on the principle of Peltier's effect. The working principle of the solar powered refrigerant is based on thermoelectric module which creates a hot side and cold side when it is supplied with electrical energy produced by the solar module. The cooler region of the thermoelectric module is used for cooling purpose while the heat produced on the hotter region is rejected to the ambient surroundings by the fans and heat sink which is the active and passive cooling method. This project is aimed to study and build a prototype of thermoelectric cooler powered by photovoltaic cell to produce refrigeration effect for cooling purpose. A simulation software (ANSYS) was used for heat transfer evaluation on the surface of the photovoltaic cell and heat flow of cooling air for analysis purpose. Water cooling method and air cooling method were applied in simulation work, then validated in experimental work. Theoretical calculation was done for the cooling load required to achieve the targeted temperature in the refrigerant area. The results showed the air cooling method provided a lower performance and achieved lower efficiency for the thermoelectric module compared to that of the water cooling method. The water cooling method produced the temperature inside the chiller box at 13°C while the temperature distributed on the surface of photovoltaic panel was 40.3°C.

Comparatively, the air cooling method produced the temperature inside the chiller box at 12.5°C while the temperature distributed on the surface of photovoltaic panel was 27.1°C. Moreover, the non cooling method produced the temperature inside the chiller box at 11.5°C while the temperature distributed on the surface of photovoltaic panel was 22.4°C

APPROVAL SHEET

This dissertation/thesis entitled "**PERFORMANCE OF THERMOELECTRIC COOLER POWERED BY PHOTOVOLTAIC CELL WITH AND WITHOUT COOLING METHOD"** was prepared by KUEK WEE EN and submitted as partial fulfillment of the requirements for the degree of Master of Engineering (Mechanical) at Universiti Tunku Abdul Rahman.

Approved by:

jun hk

_____

(Ts.Dr. Jun Hieng Kiat) Date:…1/12/2021……..
Professor/Supervisor
Department of Mechanical and Material Engineering
Faculty of Engineering and Science
Universiti Tunku Abdul Rahman

FACULTY OF ENGINEERING AND SCIENCE

UNIVERSITI TUNKU ABDUL RAHMAN

Date: _30 NOV 2021_____

SUBMISSION OF FINAL YEAR PROJECT /DISSERTATION/THESIS

It is hereby certified that **KUEK WEE EN** (ID No: ***21UEM00420***) has completed this final year thesis* entitled " **PERFORMANCE OF THERMOELECTRIC COOLER POWERED BY PHOTOVOLTAIC CELL WITH AND WITHOUT COOLING METHOD**" under the supervision of **DR. JUN HIENG KIAT** (Supervisor) from the Department of Mechanical & Material Engineering, Faculty of Engineering and Science

I understand that University will upload softcopy of my final year project / dissertation/ thesis* in pdf format into UTAR Institutional Repository, which may be made accessible to UTAR community and public.

Yours truly,

*KUEK WEE EN*
(KUEK WEE EN)

DECLARATION

I hereby declare that the dissertation is based on my original work except for quotations and citations which have been duly acknowledged. I also declare that it has not been previously or concurrently submitted for any other degree at UTAR or other institutions.

Name KUEK WEE EN

Date 30/11/2021

TABLE OF CONTENTS

Page

ABSTRACT **iii**
APPROVAL SHEET **iv**
SUBMISSION SHEET **v**
DECLARATION **vi**
LIST OF TABLES **ix**
LIST OF FIGURES

CHAPTER

1.0 INTRODUCTION

1.1 Background 1
1.2 Problem Statement 1
1.3 Objective of Project 2

2.0 LITERATURE REVIEW

2.1 Thermoelectric Module 3
2.2 Cooling system of Thermoelectric Cooler 6
2.3 Solar Photovoltaic 9
2.4 Thermoelectric Cooling System Driven by Photovoltaic System 10
2.5 Electrical and Cooling Performance of System 11
2.6 Performance of Solar Panel with Cooling Effect 13
2.7 Modelling and Simulation 15

3.0 METHODOLOGY AND WORK PLAN

3.1 Project Overview 16
3.2 Apparatus 17
3.2.1 Solar Panel 17
3.2.2 Thermoelectric Module 18
3.2.3 Heat sink with Cooling Fan 19
3.2.4 Thermal Grease 19
3.2.5 Chiller Box 20
3.2.6 Water Tubing Pipe 20
3.2.7 Portable Fan 21
3.3 Equipment 21
3.4.1 Temperature and Humidity Sensor 22
3.4.2 Infrared Thermometer 22
3.4.3 Solar Panel Charger Controller 23

3.4 ANSYS Simulation 24
3.4.1 Introduction 24
3.4.2 Steady State Thermal without Cooling Method 25
3.4.3 Air Cooling Method 26
3.4.4 Water Cooling Method 29
3.5 Experimental Work 32
3.6 Cooling Load Analysis 35

4.0 RESULT AND DISCUSSION
4.1 Introduction 39
4.2 Simulation Result 40
4.3 Experimental Result 45

5.0 CONCLUSION
5.1 Conclusion 53
5.2 Recommendation 54

6.0 REFERENCES 55

LIST OF TABLES

Table		Page
1	Performance specification of TEC1-12706	18
2	Properties of the layer of PV panel	25
3	Temperature inside chiller box and temperature on the surface of PV panel without cooling method applied	45
4	Temperature inside chiller box and temperature on the surface of PV panel with air cooling method applied	46
5	Temperature inside chiller box and temperature on the surface of PV panel with water cooling method applied	50
6	Voltage, current and COP on different cooling method	52

LIST OF FIGURES

Figures		**Page**
1	Schematic diagram of thermoelectric cooler (Ch.Sabrish 2015)	4
2	Schematic diagram of principle of Seebeck Effect (Shittu el al. 2020)	7
3	Schematic diagram of principle of Peltier Effect (Shittu el al. 2020)	8
4	Project Work Flow	16
5	30 W Monocrystalline Silicon Solar Panel (Lee 2021)	17
6	TEC1-12706 thermoelectric module	18
7	Heat sink with cooling fan	19
8	Polyfoam Chiller Box	16
9	Water tubing pipe	20
10	Portable fan for active cooling of PV panel	21
11	Temperature and Humidity sensor	22
12	Infrared Thermometer	22
13	Solar Panel Battery Charger	23
14	Main component of PV panel	24
15	Meshing of PV panel without cooling method	26
16	Meshing of PV Panel with Air Cooling	27

17	Position of Inlet and Outlet of the Airflow	28
18	Meshing of Water Tube with Water Cooling	30
19	Assemble of thermoelectric cooler with heat sink screwed with fan	32
20	Thermoelectric cooler with heat sink screwed with fan	33
21	Inside view of chiller box	33
22	Temperature distribution of solar cell without cooling method applied	40
23	Temperature distribution on top surface of PV panel without cooling method applied	41
24	Temperature distribution on top surface of PV panel with air cooling method applied	42
25	Temperature distribution on top surface of PV panel with water cooling method applied	43
26	Temperature distribution of solar cell with water cooling method applied	44
27	Temperature distribution without cooling method	47
28	Temperature distribution with air cooling method	49
29	Temperature distribution with water cooling method	51

CHAPTER 1

INTRODUCTION

1.1 Background

In these age and day, the issue of the growing energy demand and the global warming have become one of the major issues in development of energy. The consumption of energy by air conditioner required burning of natural resources for electrical generation to meet the demands, causing greenhouse effect and air pollution. Thus, the need of renewable energy is imminent in the coming years in order to solve energy crisis and improve ecological environment. Renewable energy such as solar energy can be utilized in photovoltaic cell to drive the thermoelectric cooler. Thermoelectric is used for cooling and its utilization of traditional energy source can be reduced by replacing with the photovoltaic cell without harming the environment.

1.2 Problem Statement

The portable refrigerator is easy for transportation for storing small material that needed to be kept at low temperature. As a result, a portable refrigerator that is power by solar energy which is renewable and eco friendly to the environment is the promising technology in the future time. However, the performance of photovoltaic cell is low with long operating period due to the high temperature on

the surface of the photovoltaic module. Then, the low performance of photovoltaic module affected the performance which is the cooling effect of the thermoelectric cooler. Therefore, the cooling method by using water and air are applied to lower the surface temperature of the photovoltaic module in this project.

1.3 Objectives of the Project

This project presents development, theoretical calculation and experimental analysis to improve the efficiency of the photovoltaic cell for greater temperature reduction of chiller box. The specific objectives are listed below:

I. To establish cooling effect model of photovoltaic cell.
II. To verify cooling effect on PV via FEA simulation.
III. To validate performance of TEC powered by PV with cooling effect.

CHAPTER 2

LITERATURE REVIEW

2.1 Thermoelectric Module

The history of the thermoelectric module started in 1800's when a French physicist discovered the Peltier phenomenon during his study. When the voltage is supplied to the semiconductor material, (Hao et al., 2020) stated that a temperature is formed on the surface of thermoelectric module. (Su et al., 2015) conducted experiment by supplying the electrical energy onto the Peltier module and found that the heat transfer occurred from one surface of the Peltier module to the another surface of the device. (Su et al., 2015) described the Peltier module functions like the solid state heat pump. As mentioned above, the heat and cooling effect are formed on each side of the thermoelectric module, thus, the heating or cooling effect can be reversed based on the flowing direction of the current. As a result, the thermoelectric module can be functioned as cooling or heating device by switching the polarity of the current supplied while not changing the default configuration. A study on changing the position of N-type material through electrical connector was done by (Jiang et al., 2019), aiming to validate the heat generated by thermoelectric module depends on the flowing direction of the current. (Liu et al., 2021) concluded that the heat generated by thermoelectric module reduces when the electron of the thermoelectric module consumed the thermal energy to allow the movement to the high energy state. Similarly, the effect of heat generated can be increased based on the same fundamental.

Figure 1 shows the schematic diagram of the thermoelectric cooler which illustrates the basic working principle of the thermoelectric module. The P-type and N-type semiconductor material based on the schematic diagram are sandwiched by two ceramic plate and the plate are placed on the outer area of the component. Firstly, the electrons move to the N-type material through the electrical connector departing from the P-type material. In consequence, the heat generated is reduced on the cold surface of the thermoelectric cooler when the electron started moving to the higher energy state due to the thermal energy is absorbed and carried by electron.

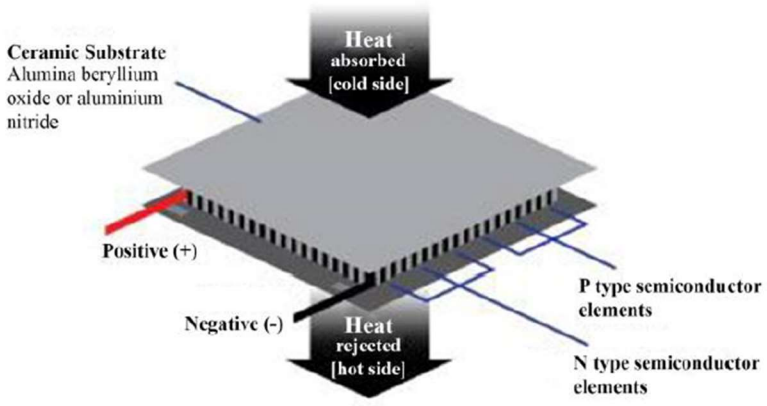

Figure 1 Schematic diagram of thermoelectric cooler (Ch.Sabarish 2015)

The major materials used for fabrication of thermoelectric are semiconductors, ceramic and polymer in which investigations and studies of material properties were performed in order to satisfy the thermoelectric properties (Hamid Elsheikh et al. 2014). Due to large value of Seebeck coefficient and thermal conductivity, the semiconductor electronic module is capable for operating period

for several years despite working under high temperature. A study was done by (Tani & Kido 2005) that ZT material is used for small bandgap semiconductor which has properties of high performance and efficiency for the thermoelectric material. The study was continued by (Mahmood et al., 2019), studying the utilization in thermoelectric module by experimenting the performance of magnesium family perovskites. In term of ceramic, silicon-germanium (SiGe) and bismuth telluride ($Bi2Te_3$) are the most common material in thermoelectric due to oxidation resistance, low toxicity and high chemical stability (Zhu et al., 2014). However, the thermoelectric performance is so low that it is unable to be used for conventional application such as huge cooling application for wide area due to limited electrical conductivity. Thus, (Sabir et al., 2019) studied the outcome of doping effect of Na and W in ceramic and concluded that doping improves the electrical conductivity and also lowers the thermal conductivity. As a result, the overall performance and efficiency of the thermoelectric module can be improved greatly. Next, the selection of polymer for thermoelectric is based on the criteria of eco-friendly and environment benign as the non-organic thermoelectric materials have property of high toxicity and high production cost. Apart of eco-friendly property, the properties of polymer for thermoelectric requires low-weight ratio, low manufacturing cost and high mechanical flexibility (Wang et al., 2011).

2.2 Cooling system of Thermoelectric Cooler

The priorities consideration during design of thermoelectric cooler (TEC) are the cooling effect that lowers the specific temperature of a certain area and the coefficient of performance (COP) of the system in order to achieve maximum cooling effect by lowering the power input to the thermoelectric cooler where the coefficient of performance can be maximized (Xuan 2003). Generally, a thermoelectric cooler system consists of thermoelectric cooler, heat sink, heat source, electrical unit and control unit. Several studies on TEC and experiments were conducted based on thermoelectric module design, thermal design and variable of operational condition of thermoelectric cooler in order to increase the COP of the TEM (Zhao & Tan 2014). (Dai et al., 2002) conducted an experiment on thermoelectric refrigerator powered by photovoltaic module and the result showed that the coefficient of performance of the experiment was 0.3 and the temperature of the cooling area was maintained from 5°C to 10°C. A similar experiment was conducted by (Min & Rowe 2006) where the COP of thermoelectric cooler ranged from 0.3 to 0.5 with the cooling temperature of 5°C at 25°C of ambient temperature. An arrangement of electrical power supply based on series and parallel method was studied by (Jugsujinda et al., 2011) and the COP resulted at 0.45.

(Saifizi et al., 2018) analysed and evaluated the cooling temperature of the hybrid TEC system that was based on uninterupted air to air heat pump. (Feng et al., 2018) investigated the change of thermoelectric generator- thermoelectric cooler (TEG-TEC) based on the Thomson effect and they found that COP of system was reduced by 18.7% and the cooling volume was reduced 27% by Thomson effect. (Feng et al., 2018) continued the study on the performance of TEG driven by thermoelectric heat pump device based on the Thomson effect. Next, (Gao et al., 2018) investigated the effect of hydrogen liquefier, Seebeck and Peltier effect on multi stage TEC. Figure 2 and 3 show the schematic diagram of Seebeck and Peltier effect. A water cooling system for multi-stage TEC that was powered by photovoltaic module was studied by (Tijani et al., 2018) and they found that the COP of system was 0.45 with the temperature changing with time resulted at 0.004°C/s.

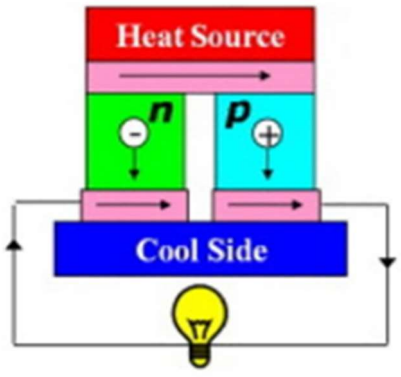

Figure 2 Schematic diagram of principle of Seebeck Effect (Shittu et al. 2020)

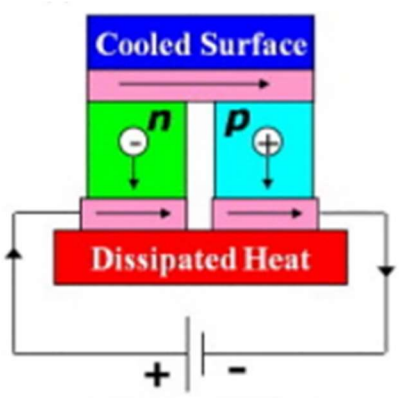

Figure 3 Schematic diagram of principle of Peltier Effect (Shittu et al. 2020)

Several studies based on the entropy generation minimization which involve the thermodynamics, heat transfer and fluids mechanics that would affect the irreversibility of the total system which involving the irremediable of fluid flow and mass transfer. An experiment based on the heat exchanger of the thermoelectric system was conducted with the optimization of heat transfer for the purpose of improving the COP of system and enlarging the cooling capacity (Luo et al. 2003). Furthermore, (Meng et al., 2010) optimized the finned heat exchanger in order to conduct and analyse of the performance and irreversibility of TEC system. The results showed that a more detail and accurate evaluation for the optimization of the system was shown by using the hybrid method of the non-equilibrium thermodynamics and finite time thermodynamics. Moreover, (Vikhor and Anatychuk 2006) evaluated the means of optimal control with various configurations for the design of TEC system and this study was continued by (Gutierrez and Mendez 2008) who contributed the work of minimization of entropy that generated in the TEC system. As the working principle of the thermoelectric

module forms heat and cold effect on each side of the surface when the power is supplied, thus heat sink that is used for heat dissipation where the heat is transfered through convection could affect the COP and performance of the TEC system. Apart from the outer heat sink, the location of the inner heat sink is one of the key factors for the chilling area due to the circulation of cooling air.

2.3 Solar Photovoltaic

Photovoltaics (PV) effect is the energy conversion done by semiconducting materials, where light energy is transformed into electricity (Li et al., 2021). Thus, electricity generation is one of the widely used application based on the fundamental of photovoltaic and also used as the photosensors. In 1839, French physicist, Edmond Becquerel conducted an experiment on a metal electrode and he discovered the photovoltaic effect during the conduction of the solution. He discovered that more electricity produced by cell during light exposure. Later in 1873, selenium that could function as a photoconductor was discovered by Willoughby Smith. In 1876, William Grylls Adams and Richard Evans Day worked on the photovoltaic principle in selenium and they showed that electricity was generated when selenium was exposed to light. An american inventor, Charles Fritz discovered the photovoltaic effect and he created the working selenium solar cell in 1883. (He et al., 2013) reported that the large-area p–n junction which is made up from the silicon is the common material available and it is known as solar cell. Other examples of solar cell types are organic solar cells , perovskite solar cells, quantum dot solar cells and

dye sensitized solar cells. (Karami Lakeh et al., 2019) reported that light is allowed by a transparent conduction film for entering into active material. Then, the generated charge carries are collected at the illuminated area of the solar cell. Generally, indium tin oxide is used for the application due to its properties of great transmittance and good electrical conductivity.

2.4 Thermoelectric Cooling System Driven by Photovoltaic System

In 1970s, research on solar refrigeration was developed and named as the 'cold chain project' by World Health Organization (WHO) and international Health Organization (Xi et al. 2007). The thermoelectric system driven by solar cell is based on the working transformation of the solar energy that converts into the electrical energy by solar cell to drive the thermoelectric cooler in order to provide cooling effect. The system operation starts as the photon that has greater band gap energy excites the electrons in the photovoltaic system when it is irradiated by sunlight (Su et al. 2015). Then, electrical energy is generated as the electrons flow through the exterior circuit. As a result, the way of using solar energy to power thermoelectric device contributes to the environment protection and meet the demand for energy conservation simultaneously (Najafi & Woodbury 2013). (Dai et al., 2003) studied the thermoelectric refrigerator driven by PV cells and found that the refrigerator temperature ranged between 5°C and 10°C. (Abdul-Wahab et al., 2009) manufactured and assembled a mobile thermoelectric refrigerator powered by solar

energy and they found out that the coefficient of performance (COP) resulted at 0.16. Then, (Liu et al., 2015) worked on the experimental study and analyzed the performance of a solar thermoelectric refrigerator and the COP is relatively higher compared to Abdul-Wahab's experiment, which was 3.01 by supplying hot water to the system. By developing the domestic thermoelectric cooling system driven by PV system, the Peltier module has a lower performance and COP compared to the conventional compressor unit because of the problem of insulation. The efficiency of thermoelectric cooler powered by solar energy system relies on the insolation, PV efficiency and refrigerator performance. Thus, performance of PV-driven thermoelectric cooling system is paramount in term of COP of the whole system.

2.5 Electrical and Cooling Performance of System

(Lv et al., 2021) studied on the effects of meteorological parameter such as effect of temperature, humidity, air speed, and sunlight exposure time to the PV-driven thermoelectric system. They found that the efficiency of electrical output reduced when the ambient temperature increased as the PV conversion performance of solar cell is affected by high working temperature. In term of wind speed, the electrical and cooling efficiency increased with the higher value of wind speed. The working temperature of system become lower during present of wind is due to the increase of the convection of heat transfer for the solar and surrounding. For the relative humidity effect, the value of the electric power produced and the cooling load

become lower when relative humidity increased. This is due to the water vapor in ambient emits larger wave radiation to atmosphere and thus spectral transmittance is affected by the precipitation. Next, the PV power generation increased when there is increase of sunshine time. Thus, the cooling power and electricity output also increased.

2.6 Performance of Solar Panel with Cooling Effect

The thermal coefficient for the photovoltaic (PV) panel can be found from the specification data sheet and it is affected by the temperature on the solar cell which is on the top surface area of the PV panel, thus, the overall performance of the system is affected. Therefore, several studies and researches were conducted by lowering the surface temperature of the solar module for performance improvement purpose. (Tang et al., 2010) applied the method of cooling by using forced air and water to lower the surface temperature of the PV panel in order to improve of the photoelectric conversion efficiency. They found that 4.7% of reduction of the temperature on PV panel contributed to 8.4% of increase of output power by cooling method by force air, while 8% reduction of temperature on PV panel contributed to 13.9% of increase of output power by cooling method by using water. (Khan et al., 2017) evaluated on water sprinkling system and active air-cooled system and found that 13.14% of maximum efficiency was produced compared to the non-cooling method. Also, they concluded that the heat sink based passive cooling method is less efficient compared to the closed loop system and forced air cooling by fan system.

(Dubey and Tiwari 2008) applied a diverse solution method to lower the surface temperature of PV panel and studied the relationship between conversion efficiency and temperature of top surface of the PV panel. Next, (Tonui and Tripanagnostopoulos 2007) conducted a similar method as Tang in which they used hybrid photovoltaic-thermal system for the cooling purpose but the water used for cooling was recirculated for home application instead of closed looping for cooling purpose only. (Sabry et al., 2018) concluded that the performance of water as cooling material for the PV panel is relatively higher and better compared to air as cooling material due to the high glazing area of the water. Apart from the active cooling method, the design and geometry of PV system could increase the overall performance of the system. (Rajaee et al., 2020) studied on the ventilated channel for cooling at the bottom area of the PV panel by using air cooling method, however, this passive cooling method is high-cost and not convenient for small scale project.

2.7 Modelling and Simulation

(Calise et al., 2011) used zero-dimensional transient simulation model to identify the optimal configuration for Solar Heating Cooling (SHC) system in TRNSYS. Further work with three SHC layouts were designed and dynamic simulation was done in TRNSYS software. Then, (Yin et al., 2013) conducted numerical and experimental analyses on a small size and mobile absorption chiller which was powered by solar cooling. The COP of chiller was 0.31 simulated by Simulink which is a model available in MATLAB. However, sudden temperature peak within the collectors in the system affect the COP during the work of Calise and Yin. Therefore, (Herrera et al., 2015) modelled a SHC control system by using prediction feature in the model in TRNSYS that provided greater performance in term of control objective. The dynamic simulation has great potential for evaluation of energy and environmental performance of SHC system, but this approach required complex theoretical assumptions and analytical equation. Thus, (Shirazi et al., 2017) proposed a multi-objective optimization of SHC configuration developed by using similar technique in which the simulation was done by coupling TRNSYS and Matlab.

CHAPTER 3

METHODOLOGY AND WORK PLAN

3.1 Project Overview

The model implementation is the construction and simulation of the respective model with refinement introduced. For the performance evaluation of photovoltaic module and thermoelectric module numerically, CFD simulation software (ANSYS Fluent 17.0) is used to study the flow field and temperature field of the model. The governing theories, formula and parameter will be established without referencing the simulation result at the initial stage. Then, a better understanding on the chronological order of the work performed is done with simulation result. Model implementation is repeated if the experimental and simulation result are not satisfactory. RNG k-ε turbulence model, a turbulence model is used to predict the temperature and concentration in the simulation.

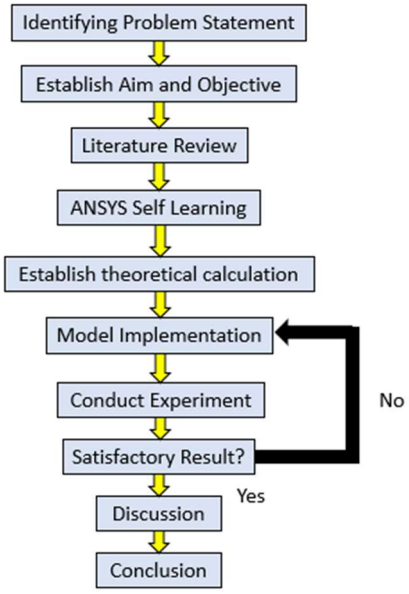

Figure 3 Project Work Flow

3.2 Apparatus

In this report, several apparatuses that are used for cooling and power supply purpose are stated below in detail with the sizing, functionality and technical specification data. These apparatuses are assembled at the stage of conducting experiment from the project work flow to determine the performance and efficiency of TEC and PV panel.

3.2.1 Solar Panel

Solar panel is the power supply for TEC, for cooling down the refrigeration volume. The material type for solar panel that was used in this project was monocrystalline silicon which has 18% to 21% of conversion rate. This solar panel is capable to deliver maximum 30 W of power at 12 V of working voltage with the dimension of 33.5*20*0.1 cm as shown in Figure 5.

Figure 5: 30 W Monocrystalline Silicon Solar Panel (Lee, 2021)

3.2.3 Thermoelectric Module

The thermoelectric module that generates heat and cold on each side of the module with the dimension of 40*40 mm is shown in Figure 6. The operating voltage for TEC1-12706 is from 0 to 15.2 V while the operating current is from 0 to 6 A. The maximum power consumption for TEC1-12706 is up to 60 W and the operating temperature is from -30°C to 70°C. Table 1 shows the data sheet for TEC1-12706.

Figure 6: TEC1-12706 thermoelectric module

Table 1: Performance specification of TEC1-12706

Hot Side Temperature (°C)	25	50
Qmax (W)	50	57
Delta Tmax (°C)	66	75
Imax (A)	6.4	6.4
Vmax (V)	14.4	16.4
Module resistance (**Ω**)	1.98	2.30

3.2.3 Heat sink with Cooling Fan

The heat sink is made up of aluminum alloy with dimension of 4.5*4*3 cm which was used for the heat dissipation from the TEC to the ambient and temperature reduction inside the cooling area. The fan with dimension of 36 mm diameter and casing with dimension of 4*4*1 cm was attached on the heat sink for applying force convection to improve the heat transfer. Figure 7 shows the heat sink that is attached with the cooling fan.

Figure 7: Heat sink with cooling fan

3.2.4 Thermal Grease

Thermal grease is used for elimination of the air gap between the heat sink and TEC so that the heat transfer and heat dissipation can be maximized to achieve greater performance of the system. The thermal conductivity of the thermal grease is 1.93 W/m-k with the capacity of 30 g.

3.2.5 Chiller Box

A chiller box with dimension of 29*17*20 cm in which the material is made up of polyfoam was used as the cooling space for the project as shown in the figure 8.

Figure 8: Polyfoam chiller box

3.2.6 Water Tubing Pipe

The water tubing pipe with dimension of 13 mm diameter as shown in figure 9 was used for transferring the water onto the PV panel to lower the surface temperature of the PV panel in order to improve the performance and COP of the system.

Figure 9: Water Tubing Pipe

3.2.7 Portable Fan

The portable fan with dimension of 14*10.6*4.2 cm that shown in figure 10 has a maximum power output of 4.5 W was used for the active air cooling for the PV panel to increase the performance of the system. The portable fan is powered by rechargeable battery and is capable to operate 5 hours with the fan blade size of 10 cm.

Figure 10: Portable Fan for active cooling of PV panel

3.3 Equipment

In this project, several equipment was used for the measurement of the experimental result and control the charger as stated below in detail with the sizing, functionality and technical specification data.

3.3.1 Temperature and Humidity Sensor

The temperature and humidity sensor shown in figure 11 with dimension of 43*43*12.5 mm was used for temperature and humidity evaluation for the area inside the chiller box in order to calculate the cooling load provided by the TEC.

Figure 11: Temperature and Humidity Sensor

3.3.2 Infrared Thermometer

The infrared thermometer shown in the figure 12 was used for the measurement of the surface temperature on the PV panel in order to evaluate the temperature difference with and without applying cooling method onto the surface.

Figure 12: Infrared Thermometer

3.3.3 Solar Panel Charger Controller

The solar changer controller shown in figure 12 was used as multi purpose solar charge and discharge controller in which the battery voltage operates at 12 V and the current charges and discharges at 30 A. The state of battery is also updated and checked by the charger controller for displaying the battery charging condition and evaluating the transporting property of pulse.

Figure 13: Solar Panel Battery Charger

3.4 ANSYS Simulation

3.4.1 Introduction

ANSYS Steady State Thermal and Fluid Flow (Fluent) was used for the determination of the surface temperature distribution on the PV panel. Firstly, ANSYS Steady State Thermal was used for analysis of the working condition of the PV panel without any cooling method applied. Figure 14 shows the main components in the PV panel which are tempered glass, encapsulant-EVA, solar cell and back sheet but the junction box which consists the diodes and connectors is ignored in this simulation work.

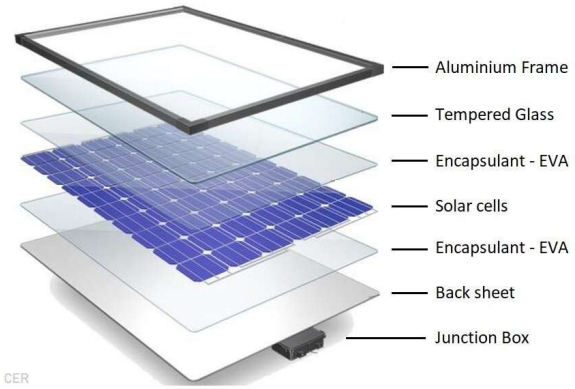

Figure 14: Main components of PV panel

The properties of the components of PV panel was imported manually into the engineering data in ANSYS based on the table below.

Table 2: Properties of the layer of PV panel

	Isotropic Thermal Conductivity (W/m.k)	Density (kg/m^3)	Specific Heat Constant Pressure (J/kg.k)
Tempered Glass	1.8	3000	500
EVA	0.35	960	2090
PV	148	2330	677
PVF	0.2	1200	1250

3.4.2 Steady State Thermal without Cooling Method

Meshing work is done on the geometry where the transition was set to slow, spin angle centre was set to fine and the smoothing quality was set to fine. Due to the license of ANSYS that run for the simulation is ANSYS student version, the limitation for the number of element and nodes generated in the simulation restrict the small element size for the element. else the total number of elements would exceed the limit. As a result, the element size was set to 10 mm instead of 2 mm. Moreover, the method of tetrahedrons was applied to the solar cell for a more detail and accurate meshing in order to obtain precise simulated result. The convection and heat flux was assumed for the steady state thermal simulation and the radiation was negligible. The film coefficient of convection was set as 10 W/m^2 °C which

was on the top and side surface area of the PV panel while the heat flux with magnitude of 800 W/m^2 was on the top surface of the PV panel. The ambient temperature of the steady state thermal simulation was kept constant at 30°C. Figure 15 shows the capture of meshing of PV panel based on the element size 0.01 m.

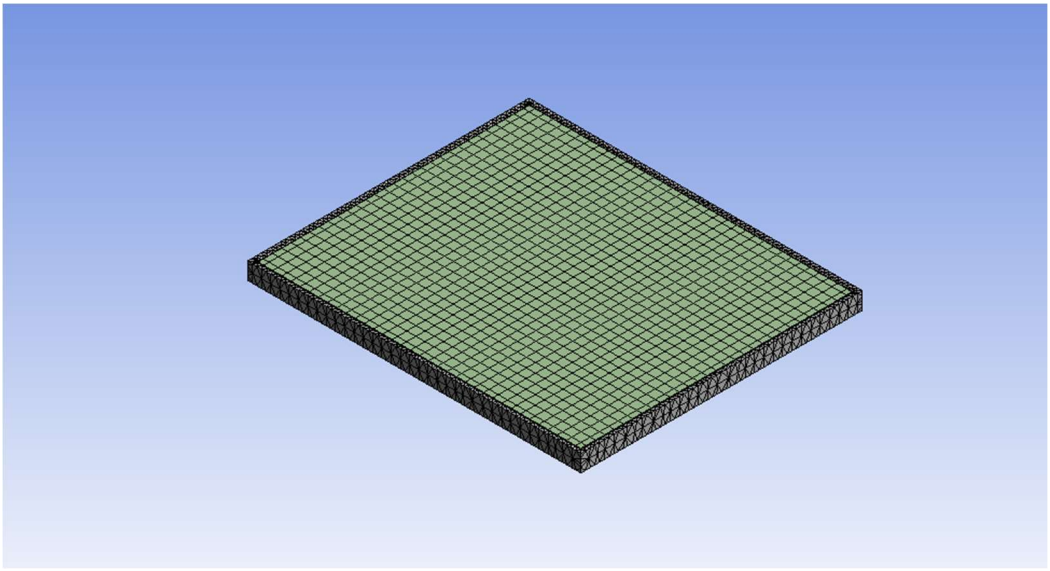

Figure 15: Meshing of PV panel without cooling method

3.4.3 Air Cooling Method

Next, for the simulation temperature distribution on PV panel with active air cooling, the element size of the meshing was set as 10 mm due to the license of ANSYS that run for the simulation is ANSYS student version, has the limitation. The method of body sizing was applied for the geometry of the PV panel with soft behavior and resulted 13,585 of nodes and 33,525 of elements generated. Also, the

method of tetrahedrons was applied to the solar cell for a more detail and accurate meshing in order to obtain precise simulated result. The meshing of PV panel is shown in figure 16.

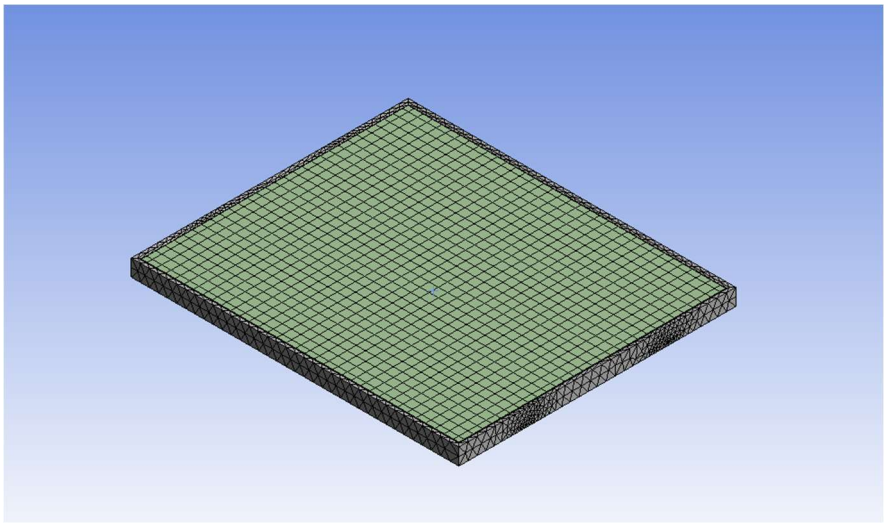

Figure 16: Meshing of PV Panel with Air Cooling

As the active air cooling method was applied on the surface of the PV panel, figure below shows the position of inlet and outlet of the air flow. The name selection was applied on the inlet and outlet for the air flow determination while the top surface of the PV panel was named for evaluation of temperature distribution after applying air cooling method on the PV panel.

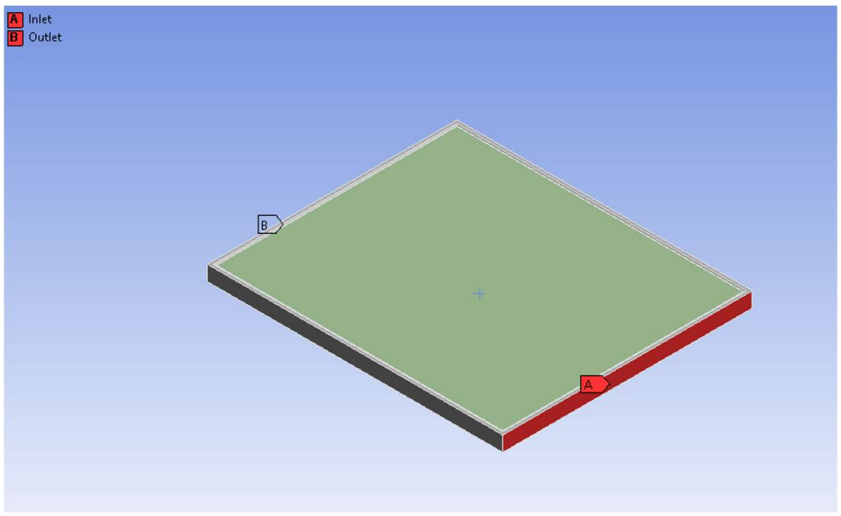

Figure 17: Position of Inlet and Outlet of the Airflow

For the model used in the simulation of air cooling on PV panel, the energy equation and k-omega SST model were applied. The model constant value of k-omega model was unchanged and applied as default value and the turbulent viscosity was not applied in this simulation. For the material of fluid, air was used for cooling method and the properties of the fluent fluid material such as density, specific heat capacity, thermal conductivity and viscosity was used in default value in fluent.

For the inlet boundary condition of air cooling simulation, the velocity specification method is the magnitude which is normal to the boundary and the reference frame is absolute. The velocity magnitude of air was flowing at 1 m/s at constant flow rate and no initial gauge pressure was applied on inlet. For the outlet boundary condition, the backflow reference frame was absolute and the gauge pressure was set to 10000 Pa. The backflow direction specification method is normal

to boundary and the backflow pressure is the total pressure of the system. In term of the thermal property, the backflow total temperature was kept constant at 303.15 K. For the wall boundary condition, the wall motion was stationary wall while the shear condition was no slip. The thermal condition of the wall was 303.15 K.

The scheme of solution method used for air cooling simulation was SIMPLE where the gradient was Least Square Cell Based, pressure was second order, momentum was second order upwind and the energy was second order upwind.

3.4.4 Water Cooling Method

Apart from air cooling method, the water cooling method was applied where the water was flowed through the surface area of the PV panel for heat dissipation purpose. The element size of the meshing was set as 10 mm due to the license of ANSYS that run for the simulation is ANSYS student version, has the limitation for the number of element and nodes generated. The method of body sizing was applied for the geometry of the PV panel with soft behavior and resulted 26,593 of nodes and 59,547 of elements generated. Also, the method of tetrahedrons was applied on the solar cell for a more detail and accurate meshing in order to obtain precise simulated result. The meshing of PV panel is shown in figure 18.

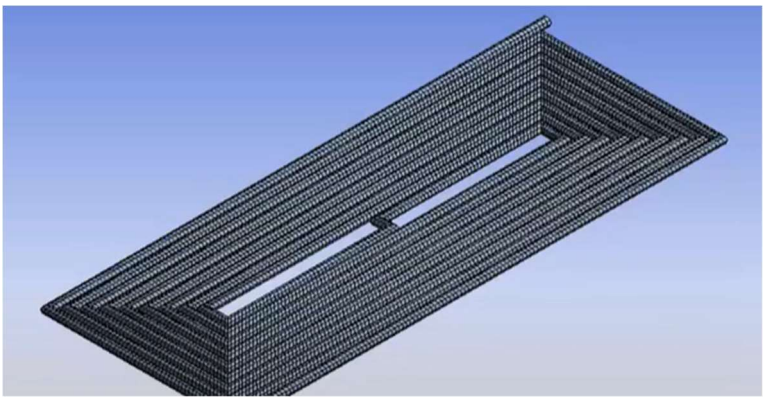

Figure 18: Meshing of Water Tube with Water Cooling

The magnitude of heat flux was 800 W/m^2 which was on the top of surface of the PV panel and the magnitude of film coefficient was 10 W/m^2K for the convection of on the body of the PV panel. Moreover, the fluid solid interface was applied on the top surface of the PV panel for the determination of temperature distribution of PV panel when the water transfer the heat away.

For the model used in the simulation of water cooling on PV panel, the energy equation and k-epsilon standard model were applied where the simulation was in steady state condition. The model constant value of k-epsilon standard model was unchanged and applied as default value and the turbulent viscosity was not applied in this simulation. Also, the enhanced wall treatment was used for the near wall treatment. For the material of fluid, water liquid was used for cooling method and the properties of the fluent fluid material such as density, specific heat capacity, thermal conductivity and viscosity were used in default value in fluent.

For the inlet boundary condition of water cooling simulation, the mass flow rate of water was set at 0.13 kg/s or also known as 0.011 ml/min at constant flow rate. The direction of the specification method was normal to boundary and the turbulent intensity was 5%. For the outlet boundary condition, the backflow reference frame was absolute and the gauge pressure was 0 Pa. The backflow direction specification method was normal to boundary with 5% of backflow turbulent intensity and the backflow pressure was the total pressure of the system. In term of the thermal property, the backflow total temperature was kept constant at 303.15 K. For the wall boundary condition, the wall motion is stationary wall while the shear condition is no slip. The thermal condition of the wall is via system coupling.

The scheme of solution method used for water cooling simulation is coupled where the gradient is Green-Gauss Cell Based, pressure was second order, momentum was second order upwind, turbulent kinetic energy was first order upward, turbulent dissipation rate was first order upward and the energy was second order upwind.

3.5 Experimental Work

The experiment setup started with the assembly work of thermoelectric cooler with the heat sink where the thermal grease were applied onto the surfaces of thermoelectric cooler for better heat transfer. One heat sink was assembled on each side of thermoelectric cooler, thus the first heat sink inside the chiller box functioned to reduce the temperature on cold side while the second heat sink that placed outside of the chiller box and functioned as receiving heat from the thermoelectric cooler and then transfering to the surrounding. Figure 19 shows the assembly of heat sink that was screwed with fan and the thermoelectric cooler. The fan is similar to the fans placed inside the chiller box. Both fans function as forced convection in order to improve the convection of the internal and external spaces of the system to improve the heat transfer.

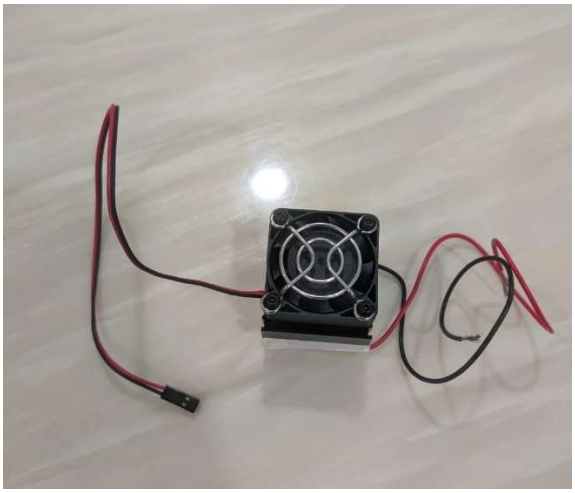

Figure 19: Assembly of thermoelectric cooler with heat sink screwed with fan

A square window was cut through the side of the chiller box to allow the placement of the thermoelectric cooler with heat sink and fan where the dimension was 4*4.5 cm. Figure 20 shows the placement of thermoelectric cooler with heat sink and fan inside the chiller box.

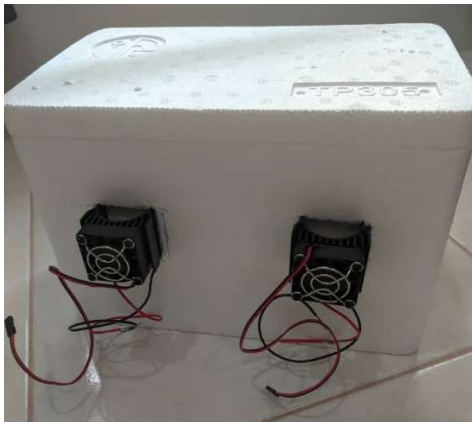

Figure 20: Thermoelectric cooler with heat sink screwed with fan

Then, the humidity and temperature sensor were placed inside the chiller box with two similar heat sinks as shown in the figure 21. Temperature was recorded for every two minutes when the experiment started.

Figure 21: Inside view of chiller box

Next, the PV panel was connected to the solar charge controller and the cable of fans and thermoelectric cooler were connected to the port available from the solar charger controller for receiving the power supply from the solar panel. Data and result were recorded and further discussion is described in Chapter 4.

3.6 Cooling Load Analysis

The calculation for the cooling power to achieve 15°C inside the chiller box is shown below where the dimension of the chiller box is 29*17*20 cm. In this project, the heat transfer for radiation was ignored, and conduction and convection of heat transfer were assumed in the calculation. The chillier box is made up of polyurethane which thermal conductivity from 0.002 to 0.035 W/mk and the surrounding temperature was presumed at 30°C for the experiment. The heat transfer for the vertical convection and horizontal convection are shown in the calculation below.

Rayleigh number (Vertical convection)

$$Ra_L = \frac{g\ \beta\ (T\infty - T)\ L^3\ Pr}{v^2}$$

$$Ra_L = 1.122\ \text{E+07}$$

Where,

g = Gravitational force

β = Volume of the expansion coefficient

T∞ = Temperature of buld

T = Temperature of wall

L = Vertical length

Pr = Prandtl number

V = Kinematic viscosity of the air

Natural convection Nusselt number

$$Nu = \left\{ 0.825 + \frac{0.387\, Ra_L^{\frac{1}{6}}}{\left[1 + \left(\frac{0.492}{\Pr}\right)^{\frac{9}{16}}\right]^{\left(\frac{8}{27}\right)}} \right\}^2$$

$$Nu = 32.355567$$

Volume of the expansion coefficient

$$\beta = \frac{1}{T_f}$$

$$\beta = 0.003384095$$

Where

T_f = temperature of film which can be calculated by dividing the sum of the surrounding temperature and temperature planned to achieve for the chiller box

Heat transfer coefficient (Vertical convection)

$$h = \frac{kNu}{L}$$

$$h = 5.6622242 \text{ W/ m}^2 \text{ °C}$$

Due to the internal and external region has the same value of heat transfer coefficient for the vertical convection, the value obtain above is similar to the value of the internal heat transfer coefficient is same as the external value.

Horizontal convection for external region.

$$h = 1.32 \left(\frac{\Delta T}{L}\right)^{\frac{1}{4}}$$

$$h = 3.539951 \text{ W/m}^2 \text{°C}$$

where

ΔT = Difference of surrounding temperature and temperature inside the chiller box

L = Length of chiller box

Horizontal convection for internal region

$$h = 0.59 \left(\frac{\Delta T}{L}\right)^{\frac{1}{4}}$$

$$h = 1.582251 \text{ W/m}^2 \text{°C}$$

Resistance of heat transfer for horizontal region

$$\frac{1}{R_1} = \frac{t}{k\, A_H} + \frac{1}{h_{Ho}\, A_H} + \frac{1}{h_{Hi}\, A_H}$$

$$\frac{1}{R_1} = 134.4581$$

where
R_1 = heat transfer coefficient on the horizontal region
t = chiller box thickness
k = thermal conductivity of chiller box
h_{Ho} = heat transfer coefficient at external region for horizontal convection
h_{Hi} = heat transfer coefficient at internal region for horizontal convection
A_H = surface area

Resistance of heat transfer (Vertical)

$$\frac{1}{R_2} = \frac{t}{k\ A_V} + \frac{1}{h_{Vo}\ A_V} + \frac{1}{h_{Vi}\ A_V}$$

$$\frac{1}{R_2} = 0.007437$$

where

R_2 = heat transfer coefficient on the vertical region
t = chiller box thickness
k = thermal conductivity of chiller box
h_{Vo} = heat transfer coefficient at external region for vertical convection
h_{Vi} = heat transfer coefficient at internal region for vertical convection
A_V = surface area of horizontal region

Total resistance for heat transfer

$$R = \frac{R_1 R_2}{R_1 + R_2}$$

$$R = 0.443918 \text{ K/W}$$

Cooling load

$$Q = \frac{\Delta T}{R}$$

$$Q = 33.79\ W$$

Where
ΔT= Temperature difference between ambient temperature and temperature inside chiller box

CHAPTER 4

RESULT AND DISCUSSION

4.1 Introduction

Chapter 4 presents the simulation and experimental result based on the temperature distribution on the surface of the PV panel. The temperature of PV panel was observed without any cooling effect applied, then with air cooling applied and lastly the PV panel was cooled with the water. The experiment was conducted which was similar to the simulation scenario i.e. no cooling method applied on the PV panel, followed by air cooling and lastly with the water cooling. Comparison of each cooling method and non-cooling method was done in this chapter.

4.2 Simulation Result

With simulation of steady state thermal, it can be seen that the temperature range of the solar cell achieved around 37°C. The center part of the solar cell has a higher value compared to the surrounding area of the solar cell. Figure 22 shows the simulation result of temperature distribution of the PV panel without cooling method applied.

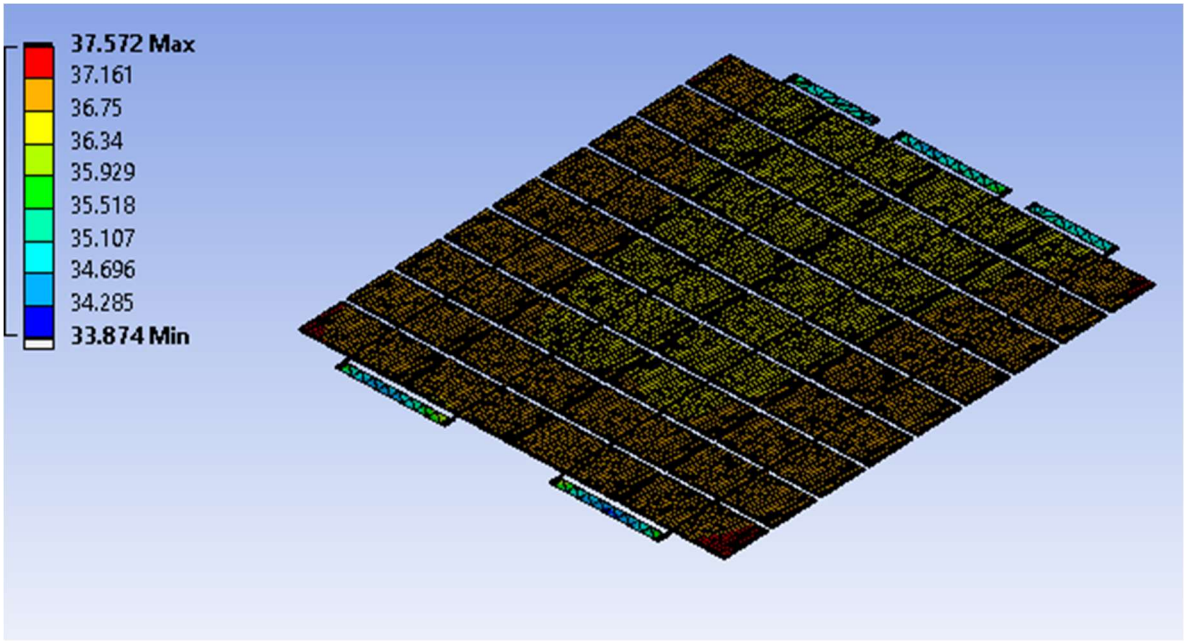

Figure 22: Temperature distribution of solar cell without cooling method applied

The temperature distribution on the top surface of the PV panel is shown in figure 23. It can be seen that most of the top surface area of the PV panel is similar which is around 39°C and a maximum of temperature of 42.87 °C is observed on the top right surface of the PV panel. The other three edges on the top surface of PV panel achieve similar temperature distribution based on the simulation results which is around 41°C.

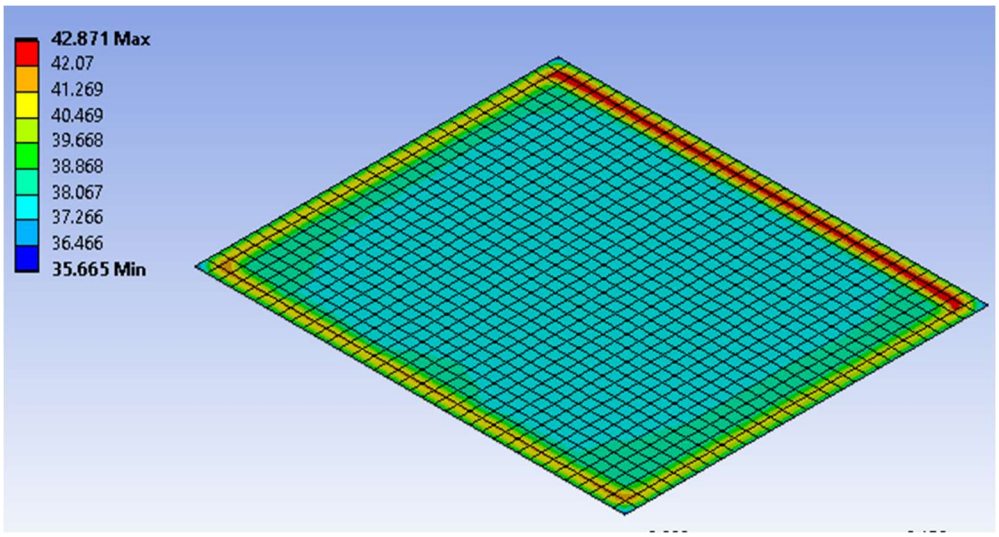

Figure 23: Temperature distribution on top surface of PV panel without cooling method applied

With simulation of fluid flow (fluent), it can be seen that the temperature range of the top surface of PV panel achieved around 300K which is 27°C. The top surface temperature distribution achieved similar result and does not have much difference compared with simulation without cooling method. Figure 24 shows the simulation result of temperature distribution of the PV panel with air cooling method applied.

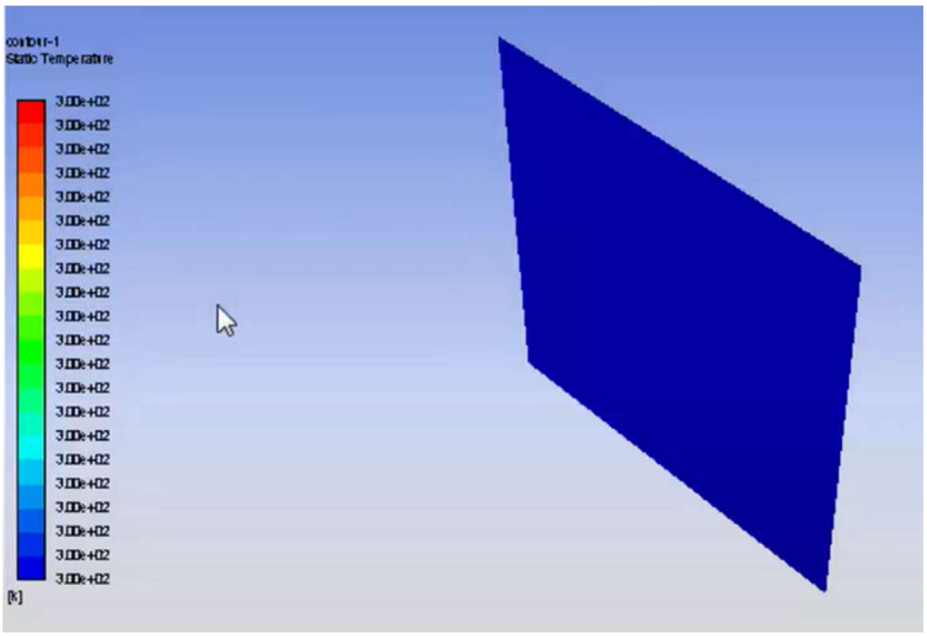

Figure 24: Temperature distribution on top surface of PV panel with air cooling method applied

With simulation of fluid flow (fluent), it can be seen that the temperature range of the top surface of PV panel achieved around 300K which is 27°C. The top surface temperature distribution achieved similar result and does not have much difference compared with simulation without cooling method. Figure 25 shows the simulation result of temperature distribution of the PV panel with water cooling method applied.

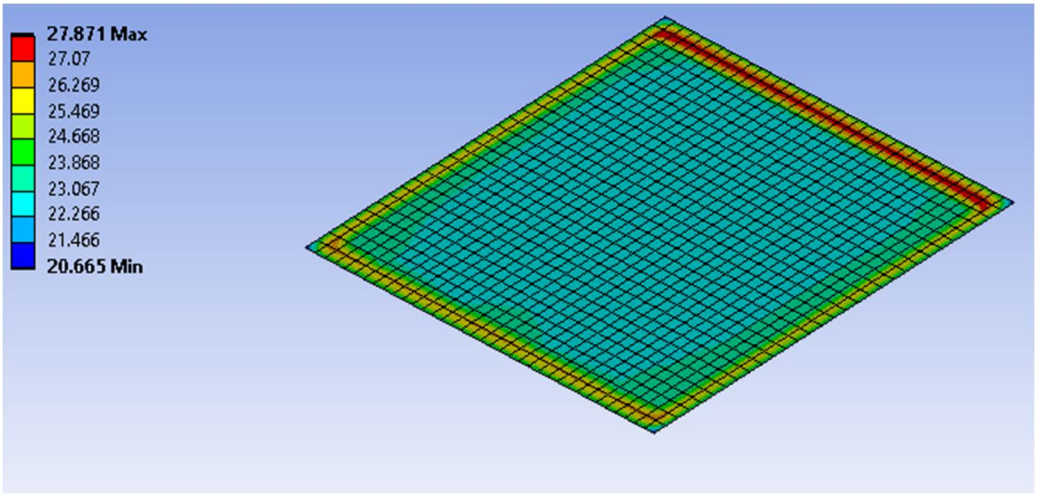

Figure 25: Temperature distribution on top surface of PV panel with water cooling method applied

Next, the temperature range of the solar cell achieved around 22°C is shown in Figure 26. The center part of the solar cell has a lower value compared to the surrounding area of the solar cell. Figure 26 shows the simulation result of temperature distribution of the PV panel with water cooling method applied.

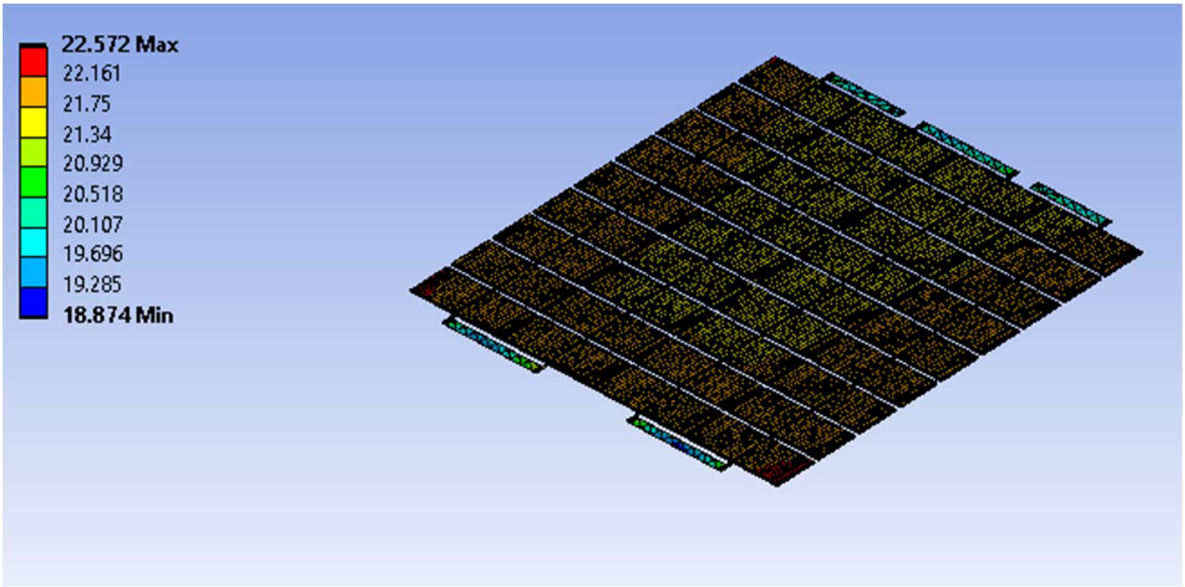

Figure 26: Temperature distribution of solar cell with water cooling method applied

Based on the three results of simulation with different cooling method for the PV panel, the temperature on the upper surface area of PV panel is reduced compared to the condition without the application of the cooling method. The water cooling method contributed the most temperature reduction on the solar cell where the center temperature of PV panel dropped from 37°C to 22°C while the temperature reduction on the top surface of PV panel dropped from 38°C to 24°C. Air cooling method also reduces the temperature on the top surface of PV panel but less than the result of water cooling method, in which the temperature dropped from

38°C to 27°C. As a result, water cooling method is more effective than air cooling method in term of reducing the temperature distribution on the top surface and solar cell which can be applied for practical application to improve the efficiency and performance of the photovoltaic module. The simulated results are then validated with the real world cases where the experiment was conducted to evaluate the mesh independent study.

4.3 Experimental Result

The experiment was conducted from 11.00 am till 3.00 pm for several days. The results of each day achieved similar pattern. Thus, result reported in this project is based on a single day. For the experiment without cooling method applied, the ambient temperature and the temperature on the top surface of the PV panel were recorded at 30°C while the temperature inside the chiller box were recorded at 27°C. Table 3 shows the temperature inside the chiller box and temperature on the top surface of PV panel without cooling method applied. Based on the experimental result, the temperature inside the chiller box is not changing and keeping constant value until 10 minutes of the experiment which is around 27°C. Then, the temperature inside the chiller box started to decrease gradually from 12 minutes of experiment period until 40 minutes of experiment period where the temperatures dropped from 27°C to 13°C. The temperature inside the chiller box keeps constant at 13°C from 40 minutes of experiment period until the end of the experiment. Next, the temperature on the surface of PV panel started to increase from 30°C gradually

until 44 minutes of experiment where the temperature reduces 40.3°C. The temperature on the surface of the PV panel keeps constant around 40.3°C until the end of the experiment. Figure 27 shows the temperature distribution without cooling method.

Table 3: Temperature inside chiller box and temperature on the surface of PV panel without cooling method applied

Time (Minutes)	Temperature inside chiller box (°C)	Temperature on the surface of PV panel (°C)
0	27.0	30.0
2	27.3	30.2
4	27.2	30.5
6	27.1	30.8
8	27.0	31.5
10	26.0	32.7
12	25.1	33.0
14	24.6	33.1
16	24.0	33.5
18	23.4	34.2
20	22.7	34.6
22	22.2	34.6
24	21.6	35.1
26	20.0	35.3
28	18.5	35.4
30	17.8	36.0
32	15.3	36.4
34	14.4	37.1
36	13.6	37.9
38	12.9	38.2
40	13.1	38.9
42	13.2	40.1
44	13.0	40.3
46	13.1	40.3
48	13.1	40.4
50	13.0	40.3
52	12.9	40.5
54	13.0	40.3
56	13.1	40.3
58	13.1	40.3
60	13.0	40.2

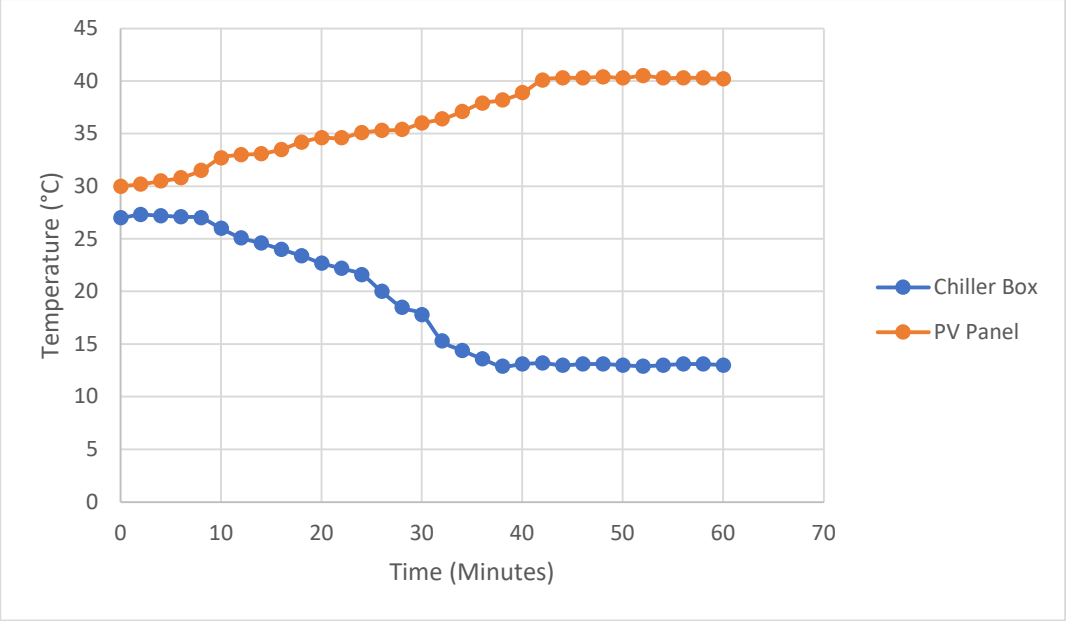

Figure 27: Temperature distribution without cooling method

For the experiment with air cooling method applied, the ambient temperature and the temperature on the top surface of the PV panel were recorded at 31°C while the temperature inside the chiller box was recorded at 28°C. Table 4 and Figure 28 show the temperature inside the chiller box and temperature on the top surface of PV panel with air cooling method applied. Based on the experimental result, the temperature inside the chiller box is not changing and keeping constant value until 8 minutes of the experiment which is around 28°C. Then, the temperature inside the chiller box started to decrease gradually from 10 minutes of experiment period until 44 minutes of experiment period where the temperatures dropped from 28°C to 12.5°C. The temperature inside the chiller box keeps constant at 12.5°C at 46 minutes of experiment period until the end of experiment. Next, the temperature on the surface of PV panel started to decrease from 31°C slowly until 36 minutes of experiment

where the temperature reaches 27.1°C. The temperature on the surface of the PV panel keeps constant around 27.1°C until the end of the experiment. Figure 28 shows the temperature distribution with air cooling method.

Table 4: Temperature inside chiller box and temperature on the surface of PV panel with air cooling method applied

Time (Minutes)	Temperature inside chiller box (°C)	Temperature on the surface of PV panel (°C)
0	28.0	31.0
2	28.0	31.0
4	28.2	30.8
6	28.1	30.7
8	28.2	30.6
10	26.2	30.5
12	25.4	30.1
14	24.8	30.1
16	24.4	30.2
18	24.0	30.3
20	23.3	30.1
22	22.7	29.8
24	21.9	29.9
26	20.1	29.5
28	19.4	28.9
30	18.6	28.6
32	18.2	28.3
34	17.7	27.6
36	16.7	27.1
38	15.9	27.1
40	14.5	27.2
42	13.8	27.0
44	12.7	27.1
46	12.5	27.1
48	12.5	27.2
50	12.4	27.1
52	12.4	27.1
54	12.4	27.0
56	12.5	27.1
58	12.5	27.1
60	12.6	27.1

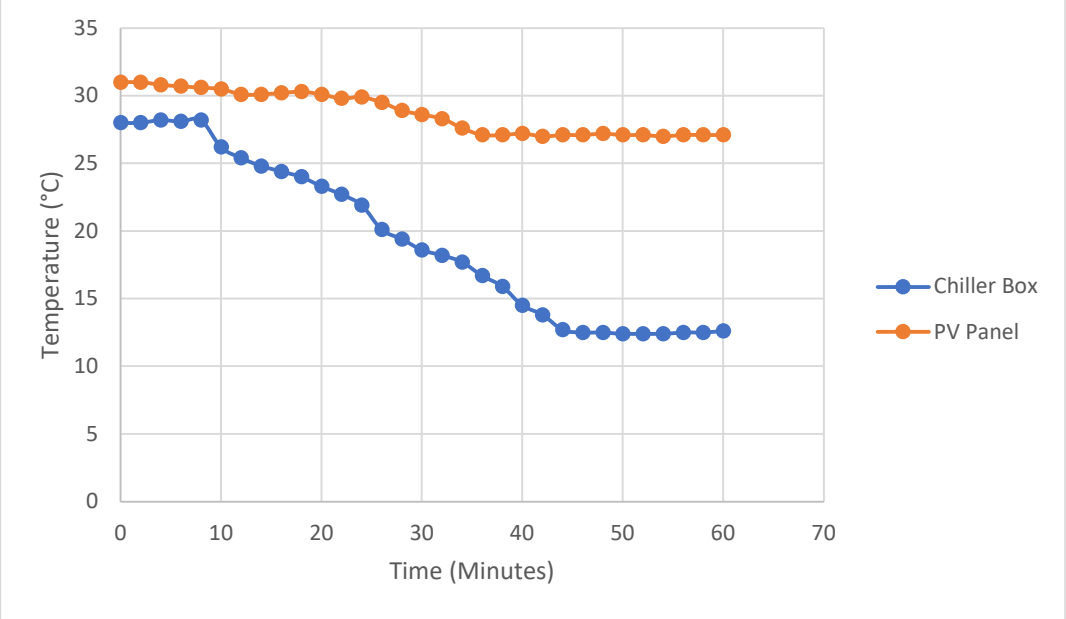

Figure 28: Temperature distribution with air cooling method

For the experiment with water cooling method applied, the ambient temperature and the temperature on the top surface of the PV panel were recorded at 31.6°C while the temperature inside the chiller box was recorded at 28.3°C. Table 5 and Figure 29 show the temperature inside the chiller box and temperature on the top surface of PV panel with water cooling method applied. Based on the experimental result, the temperature inside the chiller box is not changing and keeping constant value until 8 minutes of the experiment period which is around 28.2°C. Then, the temperature inside the chiller box started to decrease gradually from 8 minutes of experiment period until 38 minutes of experiment period where the temperatures dropped from 28.3°C to 11.6°C. The temperature inside the chiller box keeps constant at 11.6°C at 38 minutes of experiment period until the end of

experiment. Next, the temperature on the surface of PV panel started to decrease from 30.6°C slowly until 38 minutes of experiment where the temperature reaches 22.3°C. The temperature on the surface of the PV panel keeps constant around 22.4°C until the end of the experiment. Figure 29 shows the temperature distribution with water cooling method.

Table 5: Temperature inside chiller box and temperature on the surface of PV panel with water cooling method applied

Time (Minutes)	Temperature inside chiller box (°C)	Temperature on the surface of PV panel (°C)
0	28.3	30.6
2	28.3	30.1
4	28.2	29.5
6	28.3	28.9
8	28.2	28.4
10	27.5	28.0
12	27.1	27.6
14	26.8	27.3
16	26.4	26.8
18	25.9	26.1
20	24.7	25.0
22	23.2	24.1
24	21.0	23.5
26	18.9	23.3
28	17.1	22.7
30	16.0	22.5
32	14.2	22.7
34	13.5	22.6
36	12.4	22.6
38	11.6	22.3
40	11.6	22.3
42	11.5	22.4
44	11.5	22.3
46	11.5	22.2
48	11.6	22.2
50	11.6	22.3
52	11.7	22.3
54	11.6	22.5
56	11.5	22.3
58	11.5	22.3
60	11.5	22.3

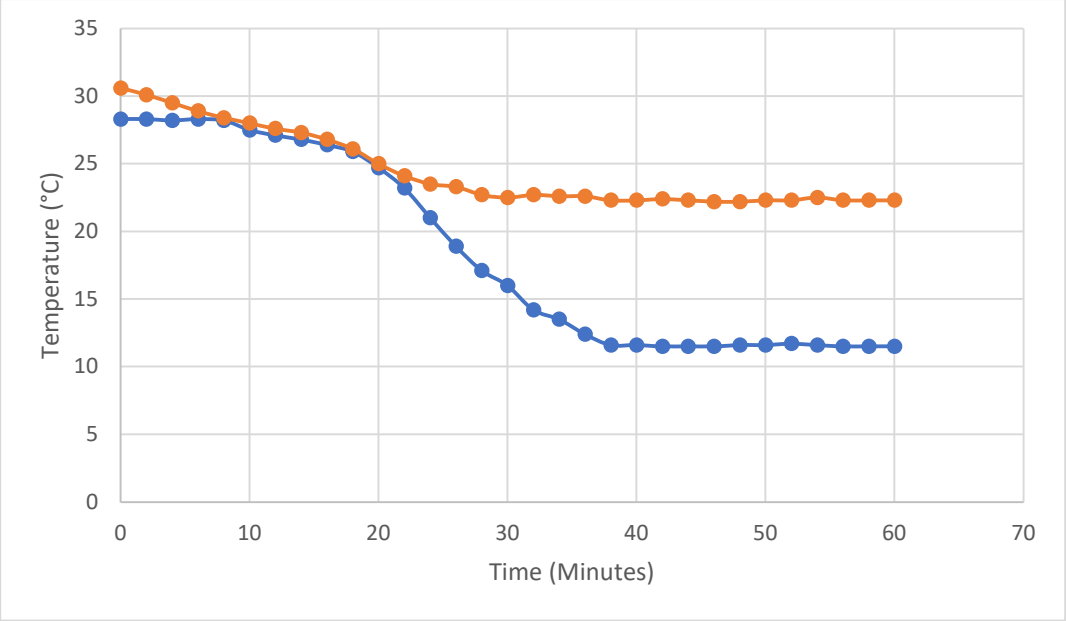

Figure 29: Temperature distribution with water cooling method

The experimental result of the water cooling method on the PV panel achieved the lowest temperature inside the chiller box and lowest temperature distribution on the surface of PV panel among the three experiments where temperature recorded at 11.6°C for the chiller box and 22.4 °C for the surface temperature of PV panel. On the other hand, the air cooling method has a relatively lower performance where the temperature for the chiller box achieved at 12.5°C and 27.1°C reported for the surface temperature for the PV panel.

Based on the experimental results, water cooling method achieve greater surface temperature reduction compared to air cooling and non-cooling method. Table 6 shows the value of voltage and current obtained from the experiment based on the different cooling methods. Coefficient of performance (COP) was performed to evaluate the effect of non-cooling and cooling method on the PV panel.

Table 6: Voltage, current and COP of PV panel on different cooling method

Method used on PV panel	Voltage, V	Current, A	Efficinecy,%
Non-cooling	11.88	0.12	2.13
Air cooling	11.89	0.19	3.37
Water cooling	11.88	0.26	4.61

Power output of PV panel wit water cooling method

$$P_{out} = V \times I$$

$$P_{out} = 11.88 \times 0.26$$

$$P_{out} = 3.088\ W$$

Power input of PV panel with water cooling method

$$P_{in} = q \times A$$

$$P_{in} = 1\ kW/m^2 \times 670\ cm^2$$

$$P_{in} = 67\ W$$

Efficiency of PV panel

$$\eta = \frac{P_{out}}{P_{in}}$$

$$\eta = \frac{3.088}{67}$$

$$\eta = 4.61\%$$

CHAPTER 5

CONCLUSION AND RECOMMENDATION

5.1 Conclusion

This work aims is to study the method on improving the performance of the photovoltaic cell that is used as the power supply for providing the electricity to the thermoelectric cooler for creating a cool ambient inside the chiller box. High temperature on the photovoltaic cell is one of the main reasons, affecting the efficiency for the system. Thus, air cooling and water cooling method are introduced by working on the simulation on ANSYS and validating via experiment.

The experimental work on the prototype of thermoelectric cooler powered by photovoltaic panel was conducted after completion of the simulation on ANSYS. Solar energy is the power supply for the thermoelectric module. In order to achieve greater performance of the thermoelectric module, heat sink and fan are used for heat dissipation for the heat to be transfered by the forced convection.

The experimental result was validated and the results were similar to the simulation work where water cooling method provided greater temperature reduction on the surface of photovoltaic panel and temperature inside the chiller box compared to the air cooling method. Water cooling has a greater level of efficiency than the air cooling as the high thermal conductivity of water that could transfer more heat and the load is diffused more efficiently. In conclusion, the result of this report provides the basic principle and comparison of water and air cooling method

on the photovoltaic cell to improve the performance and efficiency of the solar panel.

5.2 Recommendation

The software license that was used in this report was ANSYS academy which has the limitation for the number of element and nodes in the meshing section. A smaller element size can provide greater number of element and nodes which can improve the accuracy and precision of the simulation. Thus, the license key for ANSYS is recommended to be purchased for research and study in future discussion. Moreover, the insulation for the chiller box in this report can be improved by fabricating an insulated layer for better heat insulation inside the chiller box. For the accuracy and precision of the experimental result, high accuracy equipment is used for measurement instead of manual man recording. Furthermore, the cooling method can be simulated and tested in various method and the experiment should be conducted for a longer period to obtain greater accuracy and consistency of the result.

REFERENCES

Abdul-Wahab, S.A. et al., 2009. Design and experimental investigation of portable solar thermoelectric refrigerator. *Renewable Energy*, 34(1), pp.30–34.

Calise, F., D'Accadia, M.D. & Vanoli, L., 2011. Thermoeconomic optimization of Solar Heating and Cooling systems. *Energy Conversion and Management*, 52(2), pp.1562–1573. Available at: http://dx.doi.org/10.1016/j.enconman.2010.10.025.

Ch.Sabarish, R.S.R., 2015. Solar Powered Thermal Jacket For Soldiers in Extreme Temperatures. *International Journal & Magazine of Engineering, Technology, Management and Researc*, 2(June), pp.442–446.

Dai, Y., Wang, R. & Ni, L., 2002. Experimental investigation and analysis on a solar thermoelectric refrigerator. *Taiyangneng Xuebao/Acta Energiae Solaris Sinica*, 23(6), pp.754–758.

Dai, Y.J., Wang, R.Z. & Ni, L., 2003. Experimental investigation on a thermoelectric refrigerator driven by solar cells. *Renewable Energy*, 28(6), pp.949–959.

Dubey, S. & Tiwari, G.N., 2008. Thermal modeling of a combined system of photovoltaic thermal (PV/T) solar water heater. *Solar Energy*, 82(7), pp.602–612.

Feng, Y. et al., 2018. A multi-purpose electromagnetic actuator for magnetic resonance elastography. *Magnetic Resonance Imaging*, 51(April), pp.29–34. Available at: https://doi.org/10.1016/j.mri.2018.04.008.

Gómez, R. & Salvador, P., 2005. Photovoltage dependence on film thickness and type of illumination in nanoporous thin film electrodes according to a simple diffusion model. *Solar Energy Materials and Solar Cells*, 88(4), pp.377–388.

Gutierrez, F. & Mendez, F., 2008. Entropy Generation Minimization of a Thermoelectric Cooler. *The Open Thermodynamics Journal*, 2(1), pp.71–81.

Hamid Elsheikh, M. et al., 2014. A review on thermoelectric renewable energy: Principle parameters that affect their performance. *Renewable and Sustainable Energy Reviews*, 30, pp.337–355.

Hao, J. et al., 2020. Multi-parameters analysis and optimization of a typical thermoelectric cooler based on the dimensional analysis and experimental validation. *Energy*, 205, p.118043. Available at: https://doi.org/10.1016/j.energy.2020.118043.

He, W. et al., 2013. Theoretical and experimental investigation on a thermoelectric cooling and heating system driven by solar. *Applied Energy*, 107, pp.89–97. Available at: http://dx.doi.org/10.1016/j.apenergy.2013.01.055.

Herrera, E., Bourdais, R. & Guéguen, H., 2015. A hybrid predictive control approach for the management of an energy production-consumption system applied to a TRNSYS solar absorption cooling system for thermal comfort in buildings. *Energy and Buildings*, 104, pp.47–56. Available at: http://dx.doi.org/10.1016/j.enbuild.2015.06.076.

Jiang, L. et al., 2019. Thermal performance of a cylindrical battery module impregnated with PCM composite based on thermoelectric cooling. *Energy*, 188, p.116048. Available at: https://doi.org/10.1016/j.energy.2019.116048.

Jugsujinda, S., Vora-Ud, A. & Seetawan, T., 2011. Analyzing of thermoelectric refrigerator performance. *Procedia Engineering*, 8, pp.154–159. Available at: http://dx.doi.org/10.1016/j.proeng.2011.03.028.

Karami Lakeh, H., Kaatuzian, H. & Hosseini, R., 2019. A parametrical study on photo-electro-thermal performance of an integrated thermoelectric-photovoltaic cell. *Renewable Energy*, 138, pp.542–550. Available at: https://doi.org/10.1016/j.renene.2019.01.094.

Khan, M.A. et al., 2017. Performance evaluation of photovoltaic solar system with different cooling methods and a Bi-reflector PV system (BRPVS): An experimental study and comparative analysis. *Energies*, 10(6).

Li, Z., Yang, J. & Dezfuli, P.A.N., 2021. Study on the Influence of Light Intensity on the Performance of Solar Cell. *International Journal of Photoenergy*, 2021, pp.1–10.

Liu, X. et al., 2021. State of the art in composition, fabrication, characterization, and modeling methods of cement-based thermoelectric materials for low-temperature applications. *Renewable and Sustainable Energy Reviews*,

137(August 2020), p.110361. Available at: https://doi.org/10.1016/j.rser.2020.110361.

Liu, Z.B. et al., 2015. Experimental study and performance analysis of a solar thermoelectric air conditioner with hot water supply. *Energy and Buildings*, 86, pp.619–625. Available at: http://dx.doi.org/10.1016/j.enbuild.2014.10.053.

Luo, J. et al., 2003. Optimum allocation of heat transfer surface area for cooling load and COP optimization of a thermoelectric refrigerator. *Energy Conversion and Management*, 44(20), pp.3197–3206.

Lv, S. et al., 2021. A novel strategy of enhancing sky radiative cooling by solar photovoltaic-thermoelectric cooler. *Energy*, 219, p.119625. Available at: https://doi.org/10.1016/j.energy.2020.119625.

Mahmood, Q. et al., 2019. The study of mechanical and thermoelectric behavior of MgXO 3 (X = Si, Ge, Sn) for energy applications by DFT. *Chemical Physics*, 524(March), pp.106–112. Available at: https://doi.org/10.1016/j.chemphys.2019.05.009.

Meng, F., Chen, L. & Sun, F., 2010. Multiobjective analyses of physical dimension on the performance of a TEG-TEC system. *International Journal of Low-Carbon Technologies*, 5(4), pp.193–200.

Min, G. & Rowe, D.M., 2006. Experimental evaluation of prototype thermoelectric domestic-refrigerators. *Applied Energy*, 83(2), pp.133–152.

Najafi, H. & Woodbury, K.A., 2013. Optimization of a cooling system based on Peltier effect for photovoltaic cells. *Solar Energy*, 91, pp.152–160. Available at: http://dx.doi.org/10.1016/j.solener.2013.01.026.

Ni, M., Leung, M.K.H. & Leung, D.Y.C., 2008. Theoretical modelling of the electrode thickness effect on maximum power point of dye-sensitized solar cell. *Canadian Journal of Chemical Engineering*, 86(1), pp.35–42.

Rajaee, F. et al., 2020. Experimental analysis of a photovoltaic/thermoelectric generator using cobalt oxide nanofluid and phase change material heat sink. *Energy Conversion and Management*, 212(April), p.112780. Available at: https://doi.org/10.1016/j.enconman.2020.112780.

Sabir, B. et al., 2019. First principle study of electronic, mechanical, optical and

thermoelectric properties of CsMO3 (M = Ta, Nb) compounds for optoelectronic devices. *Journal of Molecular Graphics and Modelling*, 86, pp.19–26. Available at: https://doi.org/10.1016/j.jmgm.2018.09.011.

Sabry, A.H. et al., 2018. Wireless monitoring prototype for photovoltaic parameters. *Indonesian Journal of Electrical Engineering and Computer Science*, 11(1), pp.9–17.

Saifizi, M. et al., 2018. Development and Analysis of Hybrid Thermoelectric Refrigerator Systems. *IOP Conference Series: Materials Science and Engineering*, 318(1), pp.0–13.

Shirazi, A. et al., 2017. A comprehensive, multi-objective optimization of solar-powered absorption chiller systems for air-conditioning applications. *Energy Conversion and Management*, 132, pp.281–306. Available at: http://dx.doi.org/10.1016/j.enconman.2016.11.039.

Shittu, S. et al., 2020. Review of thermoelectric geometry and structure optimization for performance enhancement. *Applied Energy*, 268.

Su, S. et al., 2015. Performance evaluation and parametric optimum design of a thermoelectric refrigerator driven by a dye-sensitized solar cell. *International Journal of Refrigeration*, 60, pp.62–69. Available at: http://dx.doi.org/10.1016/j.ijrefrig.2015.07.035.

Tang, X., Quan, Z. & Zhao, Y., 2010. Experimental Investigation of Solar Panel Cooling by a Novel Micro Heat Pipe Array. *Energy and Power Engineering*, 2(3), pp.171–174.

Tani, J.I. & Kido, H., 2005. Thermoelectric properties of Bi-doped Mg2Si semiconductors. *Physica B: Condensed Matter*, 364(1–4), pp.218–224.

Tijani, I.B. et al., 2018. Development of an automatic solar-powered domestic water cooling system with multi-stage Peltier devices. *Renewable Energy*, 128, pp.416–431. Available at: https://doi.org/10.1016/j.renene.2018.05.042.

Tonui, J.K. & Tripanagnostopoulos, Y., 2007. Improved PV/T solar collectors with heat extraction by forced or natural air circulation. *Renewable Energy*, 32(4), pp.623–637.

Vikhor, L.N. & Anatychuk, L.I., 2006. Theoretical evaluation of maximum

temperature difference in segmented thermoelectric coolers. *Applied Thermal Engineering*, 26(14–15), pp.1692–1696.

Wang, L. et al., 2011. Thermoelectric properties of conducting polyaniline/graphite composites. *Materials Letters*, 65(7), pp.1086–1088. Available at: http://dx.doi.org/10.1016/j.matlet.2011.01.014.

Xi, H., Luo, L. & Fraisse, G., 2007. Development and applications of solar-based thermoelectric technologies. *Renewable and Sustainable Energy Reviews*, 11(5), pp.923–936.

Xuan, X.C., 2003. Investigation of thermal contact effect on thermoelectric coolers. *Energy Conversion and Management*, 44(3), pp.399–410.

Yin, Y.L., Zhai, X.Q. & Wang, R.Z., 2013. Experimental investigation and performance analysis of a mini-type solar absorption cooling system. *Applied Thermal Engineering*, 59(1–2), pp.267–277. Available at: http://dx.doi.org/10.1016/j.applthermaleng.2013.05.040.

Zhao, D. & Tan, G., 2014. A review of thermoelectric cooling: Materials, modeling and applications. *Applied Thermal Engineering*, 66(1–2), pp.15–24. Available at: http://dx.doi.org/10.1016/j.applthermaleng.2014.01.074.

Zhu, Y. et al., 2014. Influence of Dy/Bi dual doping on thermoelectric performance of CaMnO 3 ceramics. *Materials Chemistry and Physics*, 144(3), pp.385–389.